Characterization of the MIC/MILC Interface and Its Effects on the Performance of MILC Thin-Film Transistors

Man Wong, *Member, IEEE*, Zhonghe Jin, Gururaj A. Bhat, *Member, IEEE*, Philip C. Wong, and Hoi Sing Kwok, *Senior Member, IEEE*

***Abstract*—Process and material characterization of the crystallization of amorphous silicon by metal-induced crystallization (MIC) and metal-induced lateral crystallization (MILC) using evaporated Ni has been performed. An activation energy of about 2 eV has been obtained for the MILC rate. The Ni content in the MILC area is about 0.02 atomic %, significantly higher than the solid solubility limit of Ni in crystalline Si at the crystallization temperature of 500 °C. A prominent Ni peak has been detected at the MILC front using scanning secondary ion mass spectrometry. The MIC/MILC interface has been determined to be highly defective, comprising a continuous grain boundary with high Ni concentration. The effects of the relative locations of this interface and the metallurgical junctions on TFT performance have been studied.**

***Index Terms*—Grain boundary, MILC, nickel, thin-film transistor.**

I. INTRODUCTION

METAL induced crystallization (MIC) of amorphous silicon (a-Si) using nickel (Ni) has been achieved at a temperature (∼500 °C) [1]–[3] much lower than that (∼600 °C) typically used for solid phase crystallization (SPC) without Ni. However, the significant incorporation of Ni in the MIC polycrystalline silicon (poly-Si) films [4] might limit the potential improvement in the performance of the thin film transistors (TFT's) realized on such films. Subsequently, metal induced lateral crystallization (MILC) has been proposed [5] as a better alternative to MIC, resulting in poly-Si films with reduced Ni incorporation and large elongated grains—the long axes of which are parallel to the direction of the grain growth [4]. Low temperature TFT's with high field effect mobility have been fabricated [6]–[8], thus establishing MILC as a potentially enabling technology for realizing systems requiring low process temperature yet with high performance transistors—such as the active matrix liquid crystal displays with on-panel integrated driver circuits.

While no measurable amount of Ni has been detected within the MILC region using either transmission electron microscopy (TEM) [5], [6] or Auger electron spectroscopy (AES) [4], none of these techniques are particularly appropriate for trace element detection. Therefore, it is still not clear how Ni is distributed, from inside the MIC region, across the MIC/MILC interface, through the MILC region and finally across the MILC front to inside the a-Si region. This crucial but missing information might be particularly relevant to the unexpectedly high leakage current measured in conventional MILC TFT's [9], in which the edge of the MIC region is self-aligned to the edge of the transistor channel region. Furthermore, while the crystal grains are indeed larger in MILC poly-Si films [4], [6], the corresponding field effect mobility is still lower than those typically reported for poly-Si films obtained using laser crystallization [10] or SPC of Si implanted a-Si [11]. This suggests that the crystal grains in low temperature MILC films may be less ideal and may contain a significant number of intra-granular defects.

In this work, scanning secondary ion mass spectrometry (SIMS) and energy dispersive X-ray microanalysis (EDX) have been used to detect the distribution of Ni in laterally crystallized a-Si films. SIMS was performed on a Cameca IMS-4F platform, while TEM and EDX were performed on a Philips CM20 transmission electron microscope equipped with an Oxford Instruments ISIS EDX system. High resolution TEM has been used for crystallite defect characterization. The effects of the MIC/MILC interface on device performance have been characterized by constructing TFT's with the interface either self-aligned to or offset from the metallurgical junctions.

II. MATERIAL CHARACTERIZATION

For the material analyses, 100 nm thick a-Si films were deposited by the pyrolysis of SiH_4 at 550 °C in a low-pressure chemical vapor deposition (LPCVD) reactor. The starting substrates were either oxidized (100)-oriented silicon wafers or Corning 7059 glass coated with 500-nm thick low temperature (425 °C) LPCVD oxide (LTO). Approximately 5 nm of Ni was deposited by electron-beam evaporation on selected

Manuscript received November 30, 1999; revised November 29, 1999. This work was supported by a Competitive Earmarked Research Grant from the Research Grants Council of Hong Kong and a grant from the Hong Kong Industry Department. The review of this paper was arranged by Editor C. Y. Yang.

M. Wong and H. S. Kwok are with the Department of Electrical and Electronic Engineering, Hong Kong University of Science and Technology, Clear Water Bay, Kowloon, Hong Kong (e-mail: eemwong@ee.ust.hk).

Z. Jin was with the Department of Electrical and Electronic Engineering, Hong Kong University of Science and Technology, Clear Water Bay, Kowloon, Hong Kong. He is now with the Department of Information and Electronic Engineering, Zhejiang University, Hangzhou, China.

G. A. Bhat was with the Department of Electrical and Electronic Engineering, Hong Kong University of Science and Technology, Clear Water Bay, Kowloon, Hong Kong. He is now with the School of Engineering, Temasek Polytechnic, Republic of Singapore.

P. C. Wong is with Materials Preparation and Characterization Facility, the Hong Kong University of Science and Technology, Clear Water Bay, Kowloon, Hong Kong.

Publisher Item Identifier S 0018-9383(00)03416-X.

0018-9383/00$10.00 © 2000 IEEE

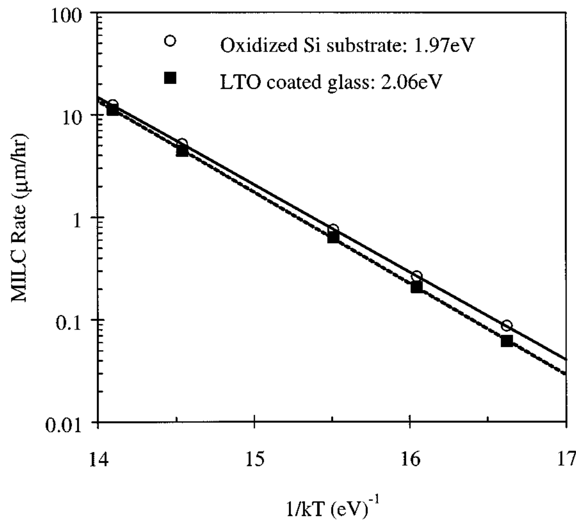

Fig. 1. Dependence of the MILC rate on the reciprocal of "kT," where "k" is the Boltzmann constant in eV/K and "T" is the heat treatment temperature in K.

a-Si regions using a photoresist masked lift-off process. The substrate temperature was maintained below 100 °C during the evaporation. Crystallization was carried out in a conventional atmospheric pressure furnace at temperature varying from 425–550 °C. The ambient during the heat treatment was high purity N_2 gas evaporated from a liquid source. The resulting MILC length was measured using an optical microscope.

The MILC rate, estimated by dividing the total MILC length by the total heat treatment time, is plotted in Fig. 1 as a function of the reciprocal of the product of the absolute crystallization temperature and the Boltzmann constant. For a given temperature, a slightly lower MILC rate has been obtained on LTO coated glass than on oxidized silicon, with activation energy (E_a) of 1.97 and 2.06 eV, respectively. These values are significantly larger than the 1.5 eV obtained for the crystallization of cosputtered a-Si(0.5% Ni) [12]. This implies the mechanism of MILC, even if not entirely different from that of the crystallization of cosputtered a-Si(0.5% Ni), may at least involve a different rate limiting step.

Ni distribution in the MIC, the MILC and the a-Si regions has been obtained using scanning SIMS. The entire area of the sample was divided into 256 sampling points. A 1 μm diameter beam of oxygen ions at 15 keV was scanned sequentially from one point to the next, with each point sputtered for about 0.9 s. A total of 500 passes were made over the collection of points, thus sputtering through the entire depth of the film at each sampling point. A two-dimensional (2-D) distribution of the integrated secondary Ni ion yield, expressed as brightness intensity, is plotted in Fig. 2. As expected, the MIC region is the brightest, indicating the highest Ni concentration. However, while no Ni was detected in the MILC region using the less sensitive AES [4], low levels of Ni, as indicated by the scattered bright spots, have been detected using SIMS. Interestingly, a dense population of bright spots also has been detected along the interface of the a-Si and the MILC regions, thus conclusively proving that the MILC front is rich in Ni. The secondary Ni ion count across a line-scan is shown in Fig. 3(a). It should be noted that the shape of this lateral Ni distribution is almost identical to that in the vertical direction [4], obtained using X-ray photo-electron spectroscopy in the MIC region. This strongly supports the proposition [4] that the MILC front is populated by a high concentration of Ni containing nodules, which are ultimately responsible for the low temperature crystallization.

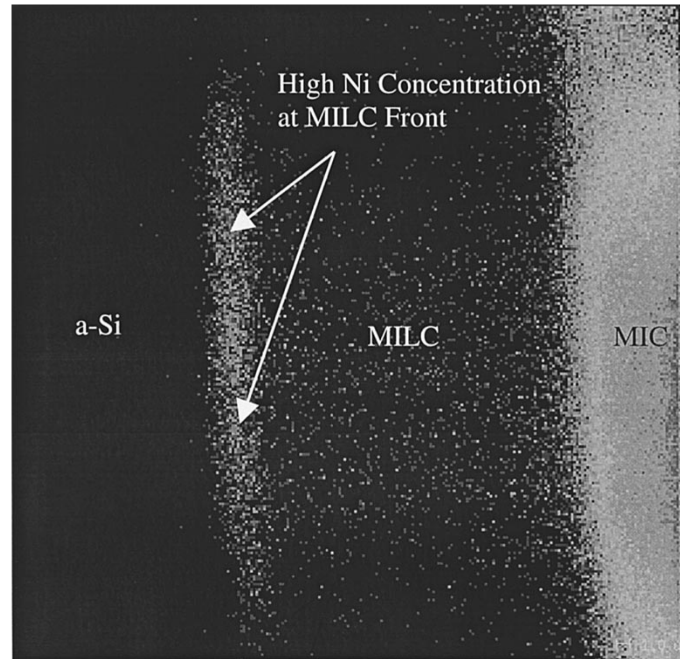

Fig. 2. Two-dimensional distribution of Ni obtained by scanning micro-SIMS analysis of the MIC, the MILC, and the a-Si regions. The Ni concentration is proportional to the brightness and the density of the spots. A high concentration of Ni, about 0.4 atom %, is observed at the MILC front.

The results of an EDX scan (5-nm spot size) across the MILC front are presented in Fig. 3(b). Since the signal near the front, though erratic, is clearly above the noise level measured in both the a-Si and the MILC silicon regions, it can be used to roughly estimate the corresponding Ni concentration. A value of 0.4 atomic % has been obtained. This value can be used to calibrate the peak of the secondary Ni ion count at the MILC front shown in Fig. 3(a). Furthermore, if it is assumed that this calibration is also valid inside the MILC region, a rough estimate of about 0.02 atomic % can be obtained for the corresponding Ni concentration. This finite concentration of Ni in the MILC region is again consistent with the proposition that slower moving Ni containing nodules would be trapped [4] in the grain boundaries in the MILC region.

A width of about 0.5 μm can be estimated from the EDX scan for the Ni rich MILC front in Fig. 3(b). The total amount of Ni within this front is roughly equal to the product of its width and the corresponding Ni concentration of 0.4 atomic %. This is just enough to supply the steady state Ni concentration of 0.02 atomic % in about 10 μm of the MILC length. Clearly, a constant supply of Ni is needed to sustain the Ni concentration at the MILC front during crystallization. This supports the proposition [13] that a continuous flux of Ni, flowing from the MIC region to the MILC front, exists inside the MILC region during steady state MILC.

A TEM micrograph showing a rugged crystallization front is presented in Fig. 4. One can observe isolated crystallized re-

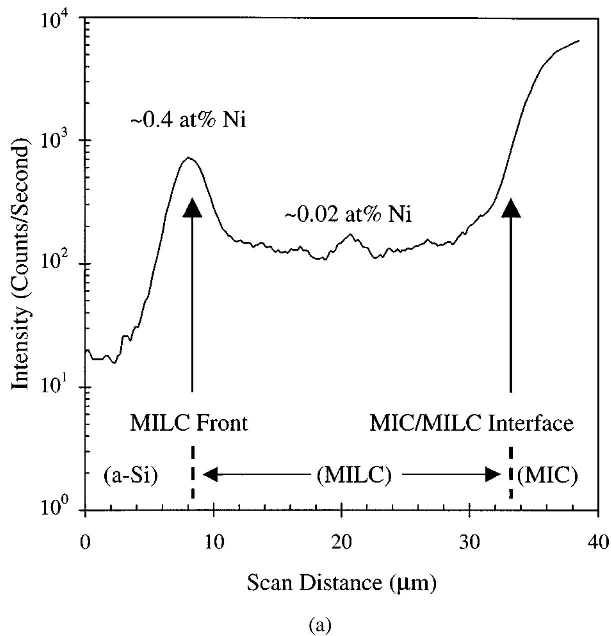

(a)

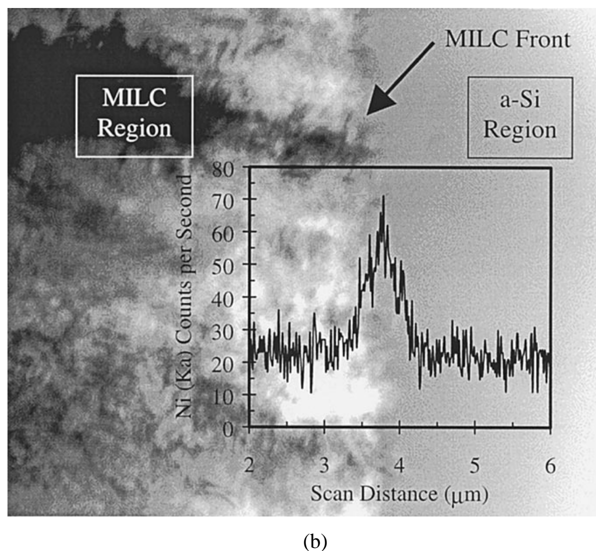

(b)

Fig. 3. Distribution of Ni across: (a) the MIC, the MILC, and the a-Si regions obtained by SIMS and (b) across the MILC front obtained by EDX.

gions, terminated by darker specs of material, protruding from the MILC region and surrounded on three sides by a-Si. The spec of material is most likely the Ni containing $NiSi_x$ nodule moving at the crystallization front and responsible for the corresponding Ni peak detected by SIMS.

A higher magnification TEM micro-graph of the MILC region is shown in Fig. 5(a). Clearly the grains are highly defective, which explains the streaks around the predominantly {110} electron diffraction pattern shown in Fig. 5(b). Some of these defects are more visible in the high resolution TEM micrograph shown in Fig. 5(c), indicating the existence of line defects and stress field induced brightness contrast. Therefore the MILC grains, while large, nevertheless contain a large number of intragranular defects. This could be the reason [14] that smaller field effect mobility has been measured on MILC-TFT's than on poly-Si TFT's fabricated on laser crystallized a-Si [10], [14] or solid phase crystallized Si implanted a-Si [11].

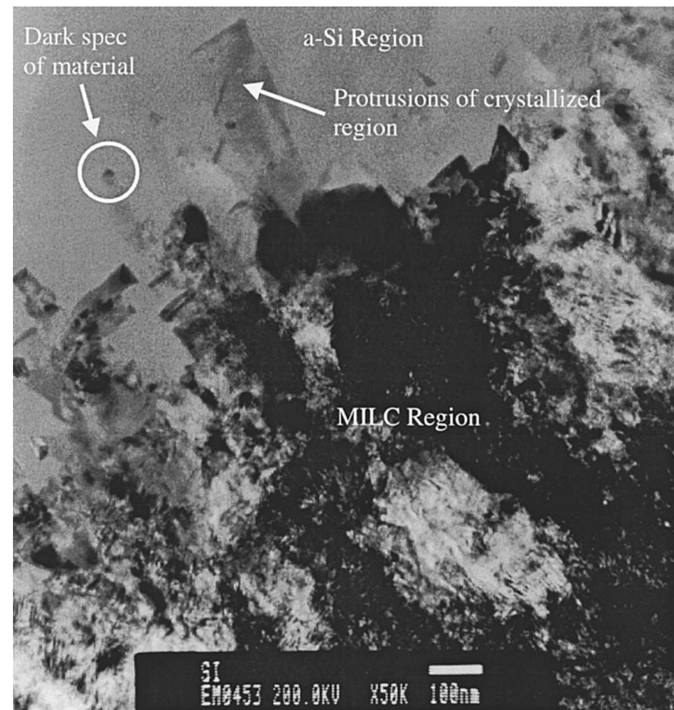

Fig. 4. TEM micrograph of a rugged MILC front. Protrusions of crystallized silicon inside the a-Si are terminated by specs of material with darker contrast.

In addition to the high Ni concentration near the MIC/MILC interface [Fig. 3(a)], a fuzzy but continuous grain boundary also coincides with this interface, as shown in the TEM micrograph in Fig. 6. It can be anticipated that such a "defective" MIC/MILC grain boundary (MMGB) would have significant electrical effects [14], [16], if placed inside the high electric field region of a reverse biased junction.

III. Discussion

The E_a value of 1.97 or 2.06 eV for the MILC rate is much larger than that of the diffusion constant of Ni either in crystalline Si (0.76 eV) [17] or in a-Si (1.3 eV) [18]. Given the proposition that MILC is an "interfacial" process mediated by Ni diffusion across $NiSi_x$ nodules at the crystallization front [4], [19], it is not surprising that neither Ni diffusion across the MILC region nor its diffusion into the a-Si region are the rate controlling steps in MILC. Interestingly, the MILC E_a values extracted from the two different kinds of substrates, while significantly different from the 1.55 eV for NiSi formation and the 2.9 eV for NiSi degradation [20], are much closer to the value of 2.08 eV for Ni induced lateral secondary grain growth in poly-Si reported by Hong *et al.* [20] and the 1.9 eV for Au induced poly-Si recrystallization reported by Allen *et al.* [21]—who suggested that the activation energy could be attributed to the energy required to attach a Si atom to the growing crystallization front.

The 0.02 atomic % Ni estimated inside the MILC region is significantly larger than the solid solubility of no more than $10^{16}/cm^3$ for Ni in crystalline silicon at 500°C [16]. Consequently, the most likely source of the secondary Ni ions detected by SIMS in the MILC region is the Ni containing nodules

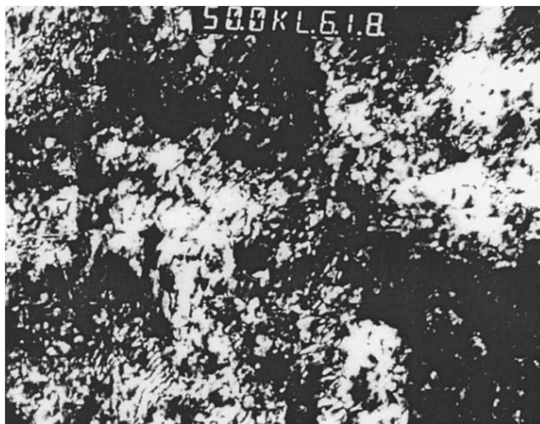

(a)

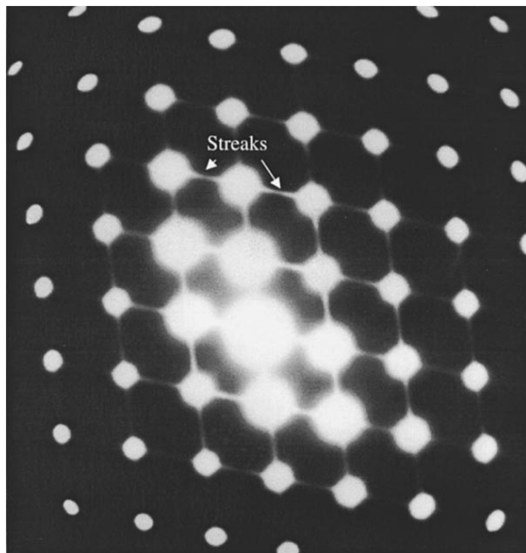

(b)

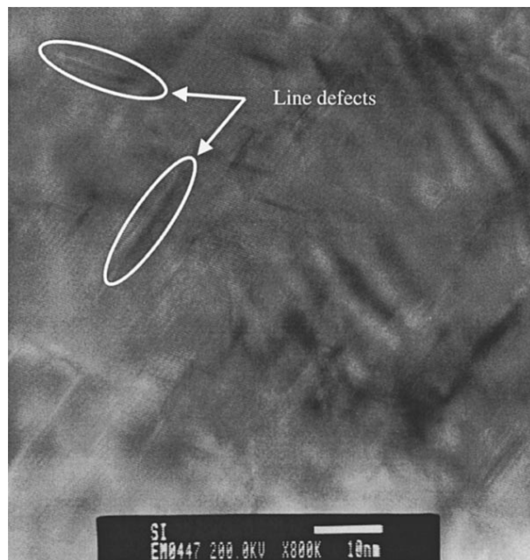

(c)

Fig. 5. Crystal quality analyses with: (a) TEM micrograph showing a high density of defects, (b) TED micrograph showing a (110) diffraction pattern. (the presence of the streaks indicates imperfections in the material), and (c) high resolution TEM micrograph showing line defects and stress field induced brightness contrast.

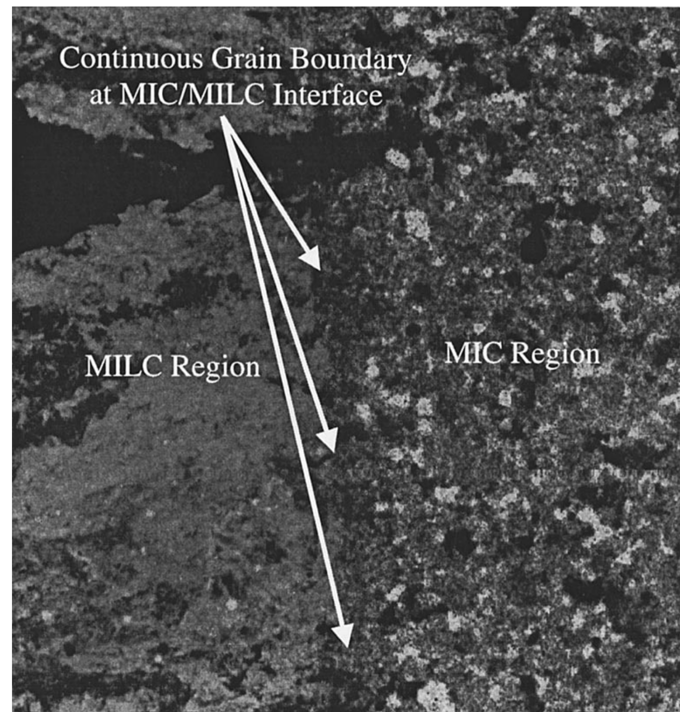

Fig. 6. TEM micrograph showing a distinct grain boundary separating the MIC and the MILC regions.

trapped in the grain boundaries [4], rather than the continuous flux of dissolved Ni in the MILC region.

IV. Device Fabrication

For studying the impact of the MIC/MILC interface on TFT performance, devices were fabricated on 100 mm silicon wafers covered with 100 nm thick thermal oxide. A thin 100 nm LPCVD a-Si layer was first deposited at respective pressure and temperature of 300 mtorr and 550 °C. After patterning the a-Si layer to form the active islands, a 100-nm thick layer of LTO gate insulator and 200-nm thick a-Si gate electrode were deposited. The wafers were thoroughly cleaned after the gate electrode patterning and the exposure of selected areas in the source and drain regions. About 2 nm of Ni was deposited in an ultra-high vacuum evaporation system. Subsequently, the source, drain, and gate regions were doped by self-aligned phosphorus implantation at a dose of 3×10^{15}/cm^2 and an energy of 40 keV. The wafers were then heat-treated at 500 °C, during which simultaneous Ni induced crystallization of the a-Si layers and dopant activation were accomplished. Finally, contact holes were opened through 500 nm of LTO insulation layer, Al-1% Si was sputter deposited and the devices were sintered in forming gas at 400 °C for 30 min. For some of the devices, hydrogen plasma passivation was performed in a 13.56 MHz parallel plate reactor at 300 °C in a 300 mtorr gas mixture of 200 sccm H_2 and 100 sccm N_2.

V. Device Characterization

Schematic cross-sections of MILC TFT's with three different MMGB locations relative to the source and drain junctions, together with the device models at low drain voltage (V_d) and

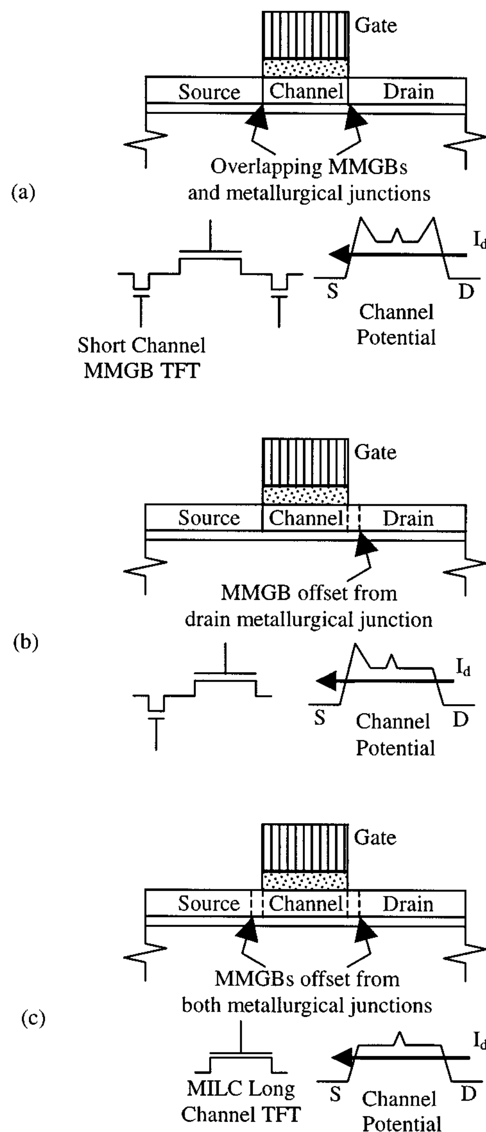

Fig. 7. Schematic cross-sections, device models at low V_d and the associated potential barriers across the channels of (a) a conventional MILC TFT with the MMGB's self-aligned to both source and drain junctions,(b) an MILC TFT with a one-sided offset, and (c) an MILC TFT with double-sided offsets.

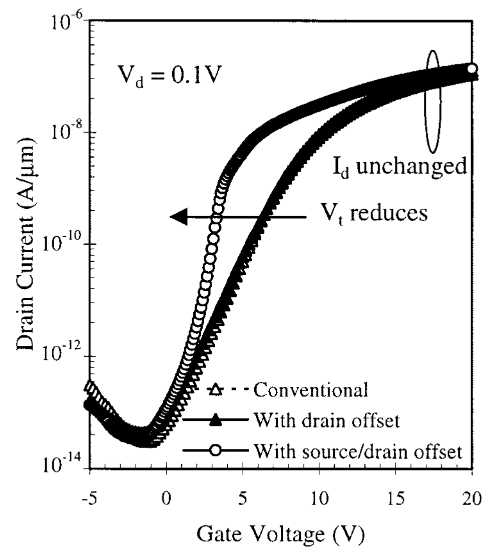

Fig. 8. I_d–V_g characteristics of the three different kinds of MILC TFT's.

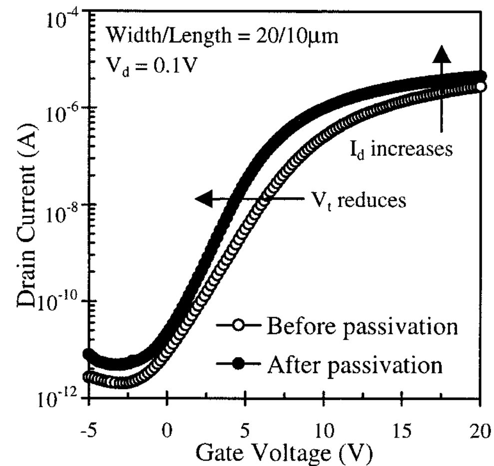

Fig. 9. Effects of plasma hydrogenation on the I_d–V_g characteristics of conventional MILC TFT's, with the MMGB's self-aligned to the metallurgical junctions.

the potential distribution across the channels, are shown in Fig. 7. Device characterization was performed at room temperature using an HP4156 Precision Semiconductor Parameter Analyzer.

Shown in Fig. 8 is the dependence of the low V_d (0.1 V) drain current (I_d) on the gate voltage (V_g) of a) a conventional MILC TFT, b) a MILC TFT with the MMGB offset from the drain-junction, and c) a MILC TFT with the MMGB's offset from both source and the drain junctions. No hydrogenation has been performed on the devices for this set of measurements. Clearly, the overall I_d–V_g characteristics and the apparent threshold voltage (V_t) of the first two devices are almost identical, where V_t is defined as the V_g needed to achieve an $I_d = W/L \times 10$ nA. W and L are the width and length of the TFT, respectively. On the other hand, the V_t value of the device with the double-sided offset is comparatively smaller.

When an MMGB coincides with any one of the metallurgical junctions, it becomes part of the channel. The high density of grain boundary trap states effectively raises the local, hence also the overall, V_t and the subthreshold slope (S) of the device. Only by removing the MMGB's from both junctions can one effectively reduce V_t and S. However, it should be noted that the difference in this V_t is only apparent and does not lead to an increase in I_d at sufficiently high V_g [22] This is because an MMGB, being a grain boundary, has a very small lateral extent. Consequently, it can be considered as a TFT with a very short channel length, albeit with a higher V_t. While conduction at low V_g is limited by such high V_t MMGB TFT [Fig. 7(a)], it is limited at high V_g by the resistance of the intrinsic MILC "long" channel TFT [Fig. 7(c)], which is common to all three device structures regardless of the locations of the MMGB's.

Clearly, the effect of the localized high-V_t MMGB TFT becomes more prominent as the channel length is reduced. This is responsible for the reverse short channel effect [23] recently

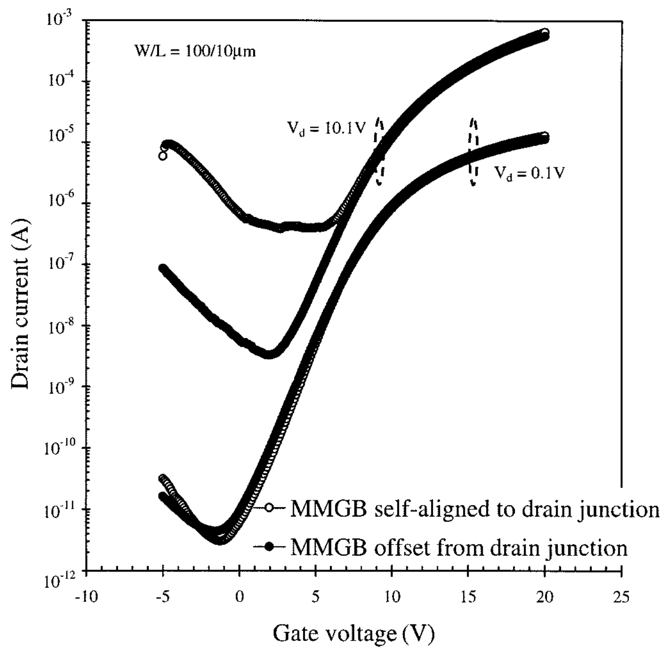

Fig. 10. Dependence of the drain current on the gate voltage. The off-state leakage current of the testing configurations with the MMGB self-aligned or offset from the drain metallurgical junctions are compared.

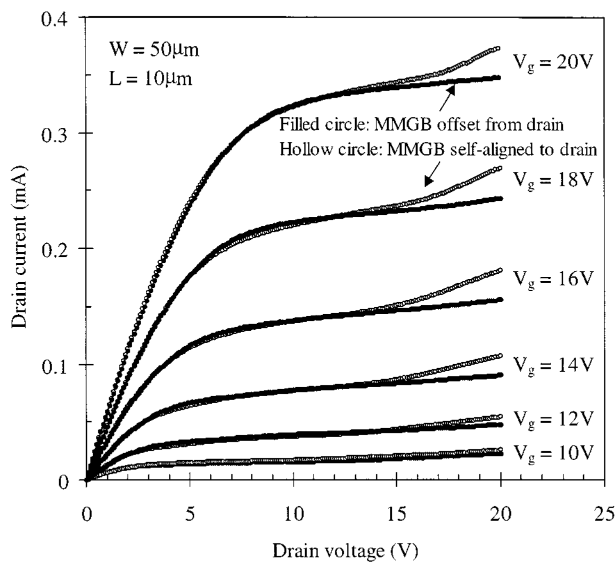

Fig. 11. Dependence of the drain current on the drain voltage at different gate voltage. Kink effects of the testing configurations with the MMGB self-aligned to or offset from the drain metallurgical junctions are compared.

reported for MILC TFT's with overlapping MMGB's and metallurgical junctions.

Since the high apparent V_t is caused by the high density of MMGB traps, it should also be possible to reduce this V_t by passivating the traps. This is demonstrated in Fig. 9. Unlike the data shown in Fig. 8, those in Fig. 9 show an increase in I_d at high V_g. This is because the MILC channel, in addition to the MMGB's, was also partially passivated by the hydrogen plasma [24].

The dependence of the I_d on V_g at high V_d (10.1 V) is shown in Fig. 10. The off-state ($V_g < 0$ V) leakage current (I_{lk}) for the testing configuration with the MMGB off-set from the drain junction is significantly lower than that for the configuration with the MMGB self-aligned to the drain junction. Since I_{lk} at high V_d is dominated by trap-assisted field-emission current, the combination of high electric field in the junction and high trap density in the overlapping MMGB will result in significantly higher I_{lk}, when compared to the case with the defective MMGB offset from the drain junction and located deep inside the quasineutral drain region [9].

Substrate current resulting from impact ionization at a sufficiently large V_d is known to lower the threshold voltage via a modulated body potential. This is manifested as current kinks in the I_d–V_d (Fig. 11) curves of the testing configuration with the MMGB self-aligned to the drain junction [25]. When the source and drain terminals are interchanged so that the MMGB is offset from the drain junction, the current kinks are suppressed. This shows that when the MMGB overlaps the drain junction, either the drain electric field or the impact ionization rate is enhanced due to the presence of charged defect states, such as the grain boundary traps or the Ni containing impurities, in the MMGB.

VI. Summary

Activation energy of 1.97 and 2.06 eV for the MILC rate has been measured on the oxidized Si and on LTO coated Corning 7059 glass substrates, respectively. A high Ni concentration has been detected at the MILC front, indicating the presence of a significant amount of Ni containing species. While the concentration of Ni inside the MILC is low, it is not negligible. The MIC/MILC interface is found to be highly defective, containing both a continuous grain boundary (MMGB) and a high concentration of Ni. The overlap of the MMGB and the drain metallurgical junction is found to have detrimental effects on the apparent threshold voltage, the leakage current and the kink-effect characteristics of MILC-TFT's. Such effects can be reduced or eliminated by separating the MMGB from the junction or by hydrogen passivation.

Acknowledgment

The authors would like to thank Dr. J. Xie for the Ni deposition, T. Smith for the SIMS analyses, Dr. K. Moulding for the TEM and EDX analyses, and Professor M. Yu for helpful discussions.

References

[1] Y. Kawazu, H. Kudo, S. Onari, and T. Arai, "Low-temperature crystallization of hydrogenated amorphous silicon induced by nickel silicide formation," *Jpn. J. Appl. Phys.*, vol. 29, pp. 2698–2704, 1990.

[2] T. J. Konno and R. Sinclair, "Metal-contact-induced crystallization of semiconductors," *Mat. Sci. Eng.*, vol. A179/A180, pp. 426–432, 1994.

[3] G. Radnoczi *et al.*, "Al induced crystallization of a-Si," *J. Appl. Phys.*, vol. 69, pp. 6394–6399, May 1991.

[4] Z. H. Jin *et al.*, "Ni induced crystallization of amorphous Si thin films on SiO_2," *J. Appl. Phys.*, vol. 84, pp. 194–200, July 1998.

[5] S. W. Lee, Y. C. Jeon, and S. K. Joo, "Pd induced lateral crystallization of amorphous Si thin films," *Appl. Phys. Lett.*, vol. 66, pp. 1671–1673, March 1995.

[6] S. W. Lee and S. K. Joo, "Low temperature poly-Si thin film transistor fabrication by metal-induced lateral crystallization," *IEEE Electron Device Lett.*, vol. 17, pp. 160–162, April 1996.

[7] G. A. Bhat, Z. Jin, H. S. Kwok, and M. Wong, "Effects of longitudinal grain boundaries on the performance of MILC- TFT's," *IEEE Electron Device Lett.*, vol. 20, pp. 97–99, Feb. 1999.

[8] Z. Jin, H. S. Kwok, and M. Wong, "Performance of thin film transistors with ultrathin MILC polycrystalline silicon channel layers," *IEEE Electron Device Lett.*, vol. 20, pp. 167–169, 1999.

[9] T. H. Ihn *et al.*, "Fabrication of metal-gate poly-Si TFT's by metal induced lateral crystallization," in *SID Dig.*, May 1997, p. 188.

[10] S. D. Brotherton, "Polycrystalline silicon thin film transistors," *Semicond. Sci. Technol.*, vol. 10, pp. 721–738, 1995.

[11] N. Yamauchi and R. Reif, "Polycrystalline silicon thin films processed with silicon ion implantation and subsequent solid-phase crystallization: Theory, experiments, and thin-film transistor applications," *J. Appl. Phys.*, vol. 75, pp. 3235–3257, April 1, 1994.

[12] T. Hempel, O. Schoenfeld, and F. Syrowatka, "Needle-like crystallization of Ni doped amorphous silicon thin films," *Solid State Communications*, vol. 85, pp. 921–924, Nov. 1993.

[13] Z. H. Jin, H. S. Kwok, and M. Wong, "The effects of extended heat treatment on Ni induced lateral crystallization of amorphous silicon films," *IEEE Trans. Electron Devices*, vol. 46, pp. 78–82, Jan. 1999.

[14] G. K. Giust and T. W. Sigmon, "High-performance thin-film transistors fabricated using excimer laser processing and grain engineering," *IEEE Trans. Electron Devices*, vol. 45, pp. 925–932, Apr. 1998.

[15] O. K. B. Lui *et al.*, "Investigation of the low field leakage current mechanism in polysilicon TFTs," *IEEE Trans. Electron Devices*, vol. 45, pp. 213–217, Jan. 1998.

[16] L. Colalongo, M. Valdinoci, and G. Baccarani, "Investigation on anomalous leakage currents in poly-TFT's including dynamic effects," *IEEE Trans. Electron Devices*, vol. 44, pp. 2106–2112, Nov. 1997.

[17] F. H. M. Spit, D. Gupta, and K. N. Tu, "Diffusivity and solubility of Ni (^{63}Ni) in monocrystalline Si," *Phys. Rev. B*, vol. 39, no. 2, pp. 1255–1260, January 15, 1989.

[18] Y. Kuznetsov and B. G. Svensson, "Nickel atomic diffusion in amorphous silicon," *Appl. Phys. Lett.*, vol. 66, no. 17, pp. 2229–2231, April 24, 1995.

[19] C. Hayzelden and J. L. Batstone, "Silicide formation and silicide-mediated crystallization of nickel-implanted amorphous silicon thin films," *J. Appl. Phys.*, vol. 73, pp. 8279–8289, 1993.

[20] Z. Hong, S. Q. Hong, F. M. Heurle, and J. M. Harper, "Thermal stability of silicide on polycrystalline Si," *Thin Solid Films*, vol. 253, pp. 479–484, 1994.

[21] L. H. Allen, J. W. Mayer, K. N. Tu, and L. C. Feldman, "Kinetic study of Si recrystallization in the reaction between Au and polycrystalline-Si films," *Phys. Rev. B*, vol. 41, pp. 8213–8220, Apr. 1990.

[22] M. Wong, G. A. Bhat, and H. S. Kwok, "Reduction of threshold voltage in metal-induced-laterally-crystallized thin film transistors," in *Proc. Asia Region Society for Information Display Symposium and Workshop*, Hsinchu, Taiwan, Mar. 17–19, 1999, pp. 281–285.

[23] ——, "Reverse short channel effect in metal-induced laterally crystallized polysilicon thin film transistors," *IEEE Electron Device Lett.*, vol. 20, pp. 566–568, November 1999.

[24] G. A. Bhat, H. S. Kwok, and M. Wong, "Plasma hydrogenation of metal-induced laterally crystallized thin film transistors," *IEEE Electron Device Lett.*, vol. 21, pp. 73–75, Feb. 2000.

[25] G. A. Bhat, Z. H. Jin, H. S. Kwok, and M. Wong, "The effects of MIC/MILC interface on the performance of MILC-TFTs," in *Dig. 56th Device Research Conf.*, June 22, 1998, pp. 110–111.

Man Wong (S'83–M'88) was born in Beijing, China. From 1979 to 1984, he studied at the Massachusetts Institute of Technology, Cambridge, where he received the B.S. and M.S. degrees in electrical engineering. From 1985 to 1988, he was at the Center for Integrated Systems at Stanford University, Stanford, CA, where he worked on tungsten gate MOS technology and received the Ph.D. degree in electrical engineering.

He then joined the Semiconductor Process and Design Center, Texas Instruments, and worked on the modeling and development of IC metallization systems and the development of dry/vapor cleaning processes. In September 1992, he joined the faculty of the Department of Electrical and Electronic Engineering, Hong Kong University of Science and Technology, Kowloon, Hong Kong. His current research interests include device fabrication technology, novel device structures and materials, thin-film transistors, display technologies and micromachines.

Dr. Wong is a member of Tau Beta Pi, Eta Kappa Nu, and Sigma Xi.

Zhonghe Jin was born in Zhejiang Province, China, in January 1970. He received the B.S., M.S, and Ph.D. degrees in 1991, 1994, and 1998, from the Department of Information Science and Electronic Engineering (ISSE), Zhejiang University, China.

From March 1996 to February 1998, he was a Visiting Scholar in the Department of Electrical and Electronic Engineering, Hong Kong University of Science and Technology, Kowloon, Hong Kong, where he was engaged in the research of low-temperature polycrystalline thin-film transistors and related materials. He is now with the ISEE Department, Zhejiang University. where he engages in the research and development of silicon-based micromachining technologies and sensors.

Gururaj A. Bhat (M'99) was born in New Delhi, India. He received the B.S. (honors) and the M.S. degrees in physics, both from the Delhi University, the M.Tech. degree in laser technology from Anna University, India, and the Ph.D. degree in 1998 from the Department of Electrical and Electronic Engineering, Hong Kong University of Science and Technology, Kowloon, Hong Kong.

After receiving the M.Tech. degree, he worked at the National Physical Laboratory, New Delhi, for two years. Currently, he is teaching at the School of Engineering, Temasek Polytechnic, Singapore. His current research interests include thin-film transistors and MEMS.

Philip C. Wong completed his graduate work at the University of British Columbia (UBC), Vancouver, B.C., Canada, where he received the Ph.D. degree in surface chemistry.

From 1988 to 1997, he worked as a Technical Manager at the Interfacial Analysis and Reactivity Laboratory, UBC, where he was also responsible for XPS, AES, and SIMS analysis in materials characterization. He joined the Materials Characterization and Preparation Facility, Hong Kong University of Science and Technology, Kowloon, Hong Kong, in 1997. Since that time, he has been working as a Senior Scientific Officer and has dealt exclusively with dynamic secondary ion mass spectrometry. During his eleven years working in surface analysis, he has been the author or co-author of more than 40 technical papers.

Hoi Sing Kwok (S'73–M'78–SM'84) received the Ph.D. degree in applied physics from Harvard University, Cambridge, MA, in 1978.

He joined the State University of New York at Buffalo in 1990 as an Assistant Professor in the Department of Electrical and Computer Engineering, and was promoted to Full Professor in 1985. He joined Hong Kong University of Science and Technology, Kowloon, Hong Kong, in December 1992, and is currently Director of the Center for Display Research. He has more than 250 refereed publications and holds more than ten patents in optics and LCD technologies.

Dr. Kwok was awarded the U.S. Presidential Young Investigator Award in 1984, and is a Fellow of the Optical Society of America. He is currently Chairman of the Society of Information Display Hong Kong Chapter.